



Research Article

New Insights from High Magnification Dermoscopy, Confocal Microscopy and Line-field Confocal Optical Coherence Tomography (LC-OCT) on Peripheral Globular Melanocytic Nevi

Arisi MariaChiara¹, Guasco-Pisani Edoardo¹, Di Lauro Francesca^{1*}, Soglia Simone¹, Perantoni Martina¹, Artelli Grazia Linda¹, Tomasi Cesare¹, Ariasi Cesare¹, La Rosa Giuseppe¹, Calzavara-Pinton Pier Giacomo¹, Licata Gaetano¹

¹Dermatology Department, University of Brescia, ASST Spedali Civili Di Brescia, P.le Spedali Civili 1, 25123, Brescia, Italy

*Correspondence author: Di Lauro Francesca, Dermatology Department, University of Brescia, ASST Spedali Civili Di Brescia, P.le Spedali Civili 1, 25123, Brescia, Italy; Email: f.dilauro@unibs.it

Citation: MariaChiara A, et al. New Insights from High Magnification Dermoscopy, Confocal Microscopy and Line-field Confocal Optical Coherence Tomography (LC-OCT) on Peripheral Globular Melanocytic Nevi. *J Dermatol Res.* 2025;6(3):1-10.

<https://doi.org/10.46889/JDR.2025.6313>

Received Date: 06-11-2025

Accepted Date: 26-11-2025

Published Date: 03-12-2025



Copyright: © 2025 by the authors. Submitted for possible open access publication under the terms and conditions of the Creative Commons Attribution (CC BY) license (<https://creativecommons.org/licenses/by/4.0/>).

Abstract

Background: The Peripheral Globular Pattern (PGN) in melanocytic nevi has traditionally been associated with benign radial growth, but its prognostic significance remains debated. The advent of new techniques offers the opportunity to refine the assessment of these melanocytic lesions.

Objectives: This study aimed to analyze the clinical, dermoscopic and imaging characteristics of PGN lesions using dermoscopy, Reflectance Confocal Microscopy (RCM) and Line-field Confocal Optical Coherence Tomography (LC-OCT).

Methods: This was a prospective, monocentric observational study conducted at the Department of Dermatology, Spedali Civili Hospital, Brescia, Italy. A total of 40 patients with at least one PGN lesion were enrolled. Dermoscopic assessments were performed at standard (10×) and high-magnification (400×), followed by RCM and LC-OCT imaging. Excised lesions were histopathologically analyzed and imaging features were statistically correlated with histopathological diagnoses.

Results: Asymmetrical globule distribution observed using conventional dermoscopy, irregular melanocyte morphology on 400x dermoscopy and atypical cellularity at RCM and LC-OCT were strong predictors of malignancy.

Conclusion: This study demonstrates that PGN lesions are not universally benign and that specific dermoscopic and high-resolution imaging features can help differentiate atypical nevi and melanomas from benign nevi. A multimodal imaging approach should be incorporated into clinical practice to enhance early melanoma detection while minimizing unnecessary excisions.

Keywords: Peripheral Globular Pattern; Melanocytic Nevi; Dermoscopy; Reflectance Confocal Microscopy; Line-field Confocal Optical Coherence Tomography (LC-OCT); Melanoma Diagnosis; High-Resolution Imaging

Introduction

Melanocytic nevi are common benign proliferations of melanocytes, frequently observed in young individuals. Among the various dermoscopic patterns, the peripheral globular pattern is often considered a hallmark of growing nevi. This pattern is characterized by the presence of pigmented globules at the periphery of the lesion, corresponding histologically to junctional nests of melanocytes arranged at the lesion's edges. Traditionally, peripheral globules have been regarded as an indicator of benignity. However, recent literature has suggested that they might also be present in melanomas [1]. Despite its clinical relevance, the differentiation between benign and malignant melanocytic lesions displaying a peripheral globular pattern remains challenging. While conventional dermoscopy provides valuable insights, new high-resolution imaging techniques, such as high-magnification (400×) dermoscopy, Reflectance Confocal Microscopy (RCM) and Line-Field Confocal Optical Coherence Tomography (LC-OCT), offer a more detailed assessment of skin lesions. However, data on the application of these technologies specifically in nevi with a peripheral globular pattern remain limited [1-3]. Given the increasing incidence of melanoma and the continuous advancements in non-invasive diagnostic techniques, a comprehensive study evaluating the dermoscopic, RCM and

LC-OCT features of melanocytic nevi with a peripheral globular pattern is crucial.

Study Objectives

The primary objective of this study is to analyze the clinical and imaging characteristics of melanocytic nevi with a peripheral globular pattern using standard dermoscopy (low-magnification and high-magnification 400×), Reflectance Confocal Microscopy (RCM) and Line-Field Confocal Optical Coherence Tomography (LC-OCT). The secondary objectives include identifying key indicators that differentiate benign from malignant lesions evaluating the relative utility of each imaging technique in diagnosing melanocytic lesions with a peripheral globular pattern and correlating imaging findings with histopathological outcomes of excised lesions.

Materials and Methods

This study was designed as a prospective, monocentric, observational and non-profit pilot study conducted at the Department of Dermatology and Venereology, Ospedali Civili Hospital, Brescia, Italy. The study aimed to build an image database and assess clinical and imaging characteristics of melanocytic nevi with a peripheral globular pattern using standard and high-resolution imaging techniques [4]. The study included adult patients (>22 years old) with melanocytic nevi displaying a peripheral globular pattern under dermoscopy. Patients were recruited between February 16, 2023 and September 30, 2023. Inclusion criteria included age ≥22 years, presence of at least one melanocytic nevus with a peripheral globular pattern and ability to provide informed consent. Exclusion criteria included a history of cutaneous melanoma, presence of extensive skin lesions preventing accurate imaging acquisition, use of immunosuppressive therapies or history of autoimmune skin diseases and any condition preventing adequate follow-up. Patients were divided in three group depending on age: group I (aged less than 30 years old), group II (aged between 30 and 50 years old) and group III (aged more than 30 years old). All enrolled patients underwent comprehensive dermatological and imaging evaluations. Lesions were assessed using three non-invasive diagnostic techniques: dermoscopy (low- and high-magnification 400×), Reflectance Confocal Microscopy (RCM) and Line-Field Confocal Optical Coherence Tomography (LC-OCT). Dermoscopic analysis was performed using a polarized digital dermatoscope (FotoFinder Vexia Medicam 1000, FotoFinder Systems GmbH, Bad Binrbach, Germany). The 10x magnification digital dermatoscope was used in order to determine globules distribution and variability in terms of pigmentation, shape and size. The 400x magnification dermoscopy was used to determine melanocytes shape (round, dendritic, round and dendritic or round and irregular). RCM was performed using a VivaScope 3000 (MAVIG, Munich, Germany), enabling *in-vivo* microscopic analysis of the epidermis and upper dermis with cellular-level resolution. LC-OCT (DeepLive DAMAE Medica, Paris, France) was used to obtain cross-sectional and en-face images of the lesions, allowing a deeper evaluation of the skin layers [5]. Both techniques were used to determine the presence of atypical cells in the lesions. For lesions meeting excision criteria, surgical removal was performed following standard dermatologic procedures. Histological examination was conducted by an expert dermatopathologist blinded to the imaging findings. Specimens were processed using hematoxylin and eosin (H&E) staining and key parameters such as melanocytic atypia, mitotic index and presence of pagetoid spread were evaluated [6].

Ethical Approval

All patients gave their consent to the study which was approved by the Local Ethics Committee Protocol Number 2688.

Statistical Analysis

All statistical analyses were conducted using IBM-SPSS® version 27.1. Data were initially structured and preprocessed using Microsoft Excel® version 365 before being imported for analysis. Continuous variables were tested for normality using the Kolmogorov-Smirnov test. Variables following a normal distribution were expressed as mean ± Standard Deviation (SD) and were compared using the independent t-test, while non-normally distributed variables were analyzed using the Mann-Whitney U test. Categorical variables were reported as frequencies and percentages. Associations between categorical variables and histopathological outcomes were analyzed using the chi-square test, with Fisher's exact test applied when expected frequencies were below five. To evaluate the diagnostic performance of each imaging modality, sensitivity, specificity, Positive Predictive Value (PPV) and Negative Predictive Value (NPV) were calculated. Receiver Operating Characteristic (ROC) curve analysis was performed for each modality. Correlation analyses were conducted to explore the relationship between key imaging parameters and histopathological outcomes. Pearson's correlation coefficient was used for normally distributed continuous variables, while Spearman's rank correlation coefficient was applied to non-normally distributed variables. To further refine the identification of malignant lesions, a multivariate logistic regression model was constructed. This model accounted for potential confounding

variables such as patient age, lesion diameter and anatomical location. Independent predictors of malignancy were identified and results were reported as adjusted Odds Ratios (OR) with 95% Confidence Intervals (CI).

For cases with available follow-up data, Kaplan-Meier survival curves were generated to assess the likelihood of lesion progression over time. The model incorporated variables such as imaging findings, patient demographics and histopathological classification, with results expressed as Hazard Ratios (HR) and 95% CI. Statistical significance was set at $p < 0.05$ for all analyses. To ensure robustness, sensitivity analyses were performed, stratifying results based on lesion size, anatomical location and patient age.

Results

This prospective, monocentric study included 40 patients, whose demographic data are reported in Table 1. Histopathologic examination after surgical excision of the PGN showed the diagnoses reported in Table 2; in particular 1 patient (2.5%) was diagnosed with severely dysplastic nevus and 1 patient (2.5%) with melanoma, both were aged more than 50 years old; most of the patients diagnosed with compound nevi belonged to age group I. The chi-square value was 8,296 and the p-value was 0,405 (Table 2).

Concerning the dermoscopic features of PGN, globules asymmetrical distribution was noted in 1 patients (16.7%) in age group I, 3 patients (3.0%) in age group II and 2 patients (20.0%) in age group III. Dermoscopic globules variability was assessed in shape, size and pigmentation. However, none of the respective correlations with age reached statistical significance (p-values = 0.594, 0.918 and 0.659, respectively) (Table 3).

High-magnification dermoscopy (400x) revealed that most patients had round, regular melanocytes. In one patient, belonging to the age group II (4.2%), were found dendritic melanocytes, while in one patients aged more than 50 years old (10.0%) were found round and irregular meanocytes. High-magnification dermoscopy showed round and dendritic melanocytes in 1 patient (16.7%) in age group I, one patient (4.2%) in age group II, 2 patients (20.0%) in age group III (chi-square = 6.142, df = 6, p = 0.407) (Table 4).

LC-OCT analysis showed atypical cellularity in 5 patients: none under 30, 3/24 (12.5%) aged 30–50 and 2/10 (20.0%) over 50 (chi-square = 1.371, df = 2, p = 0.504). RCM evaluation identified atypical cells in 8 patients: 1/6 (16.7%) under 30, 5/24 (20.8%) aged 30–50 and 2/10 (20.0%) over 50 (chi-square = 0.052, df = 2, p = 0.974) (Table 4).

We also evaluate correlations between histopathologic diagnosis and dermoscopic and imaging features. Asymmetric distribution of peripheral globules was significantly associated with more severe diagnoses, such as melanoma and severely dysplastic nevus (chi-square = 15.948, df = 4, p = 0.003) (Table 5). Other correlations (e.g., eccentric distribution, peripheral globules, variability in size, shape, pigmentation) did not reach statistical significance. However, irregular melanocyte morphology at 400x was significantly associated with melanoma (chi-square = 51.922, df = 12, p < 0.001). Table 6 as was atypical cellularity in LC-OCT (chi-square = 17.295, df = 4, p = 0.002) and RCM (chi-square = 14.479, df = 4, p = 0.006) (Table 7). A significant correlation between melanocyte variability and atypical cellularity detected via LC-OCT was found (chi-square = 8.134, df = 3, p = 0.043) (Table 7). Lastly, a strong correlation was observed between atypical cellularity on LC-OCT and that on RCM. Of the 5 patients with atypical LC-OCT findings, all (100%) also had atypical RCM features (chi-square = 22.857, df = 1, p < 0.001) (Table 6, Fig. 1-6).

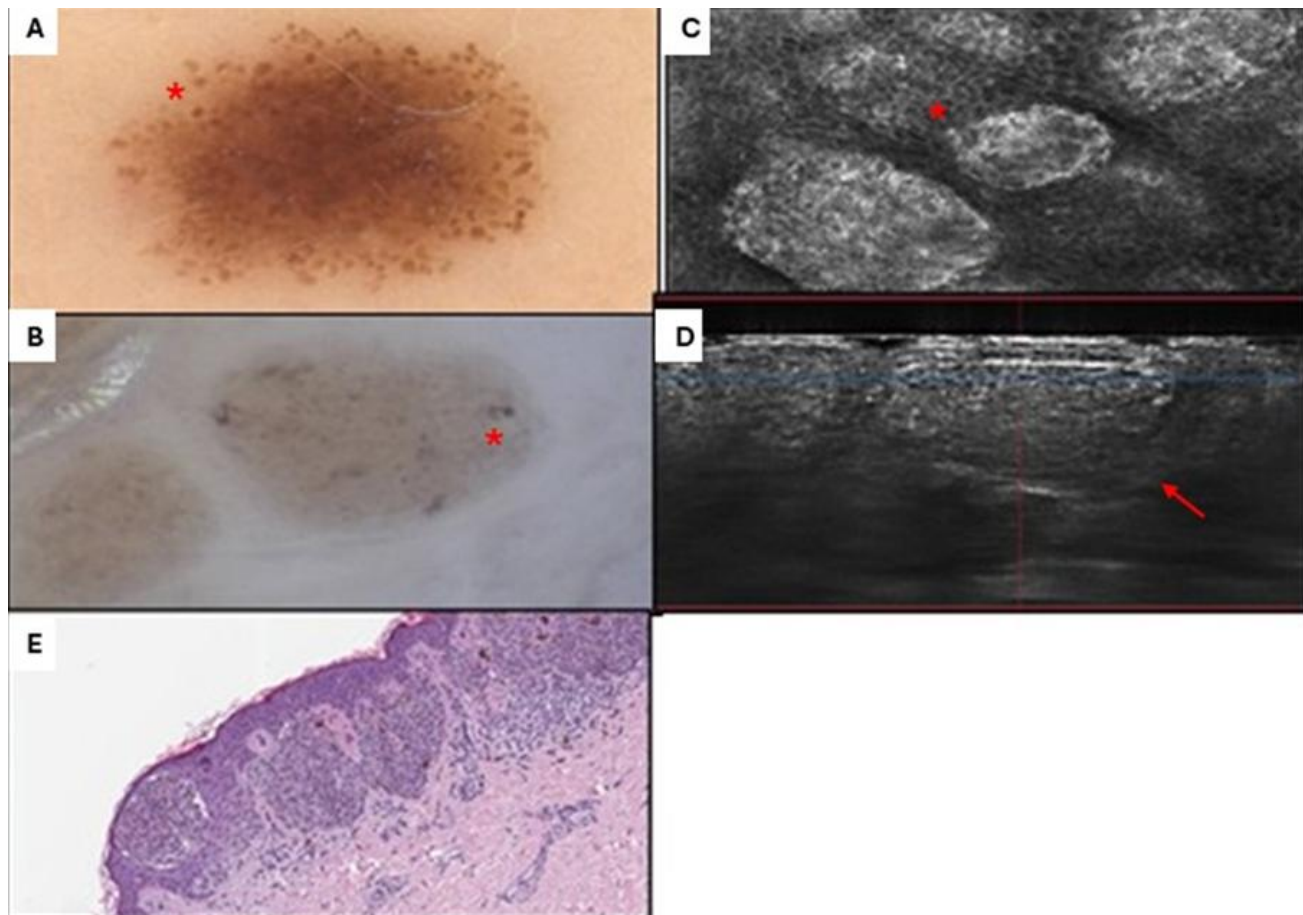


Figure 1: Compound nevi. A. 20x dermoscopy, symmetrical peripheral globules are visible, characterized by regular shape, size and pigmentation (red asterisk) B. 400x dermoscopy. Melanocytes organized in regular nests (red asterisk) C. RCM. Melanocytes organized in regular nests (red asterisk) D. LC-OCT, absence of atypical cells and well-defined epidermal junction (red arrow) E. Histology.

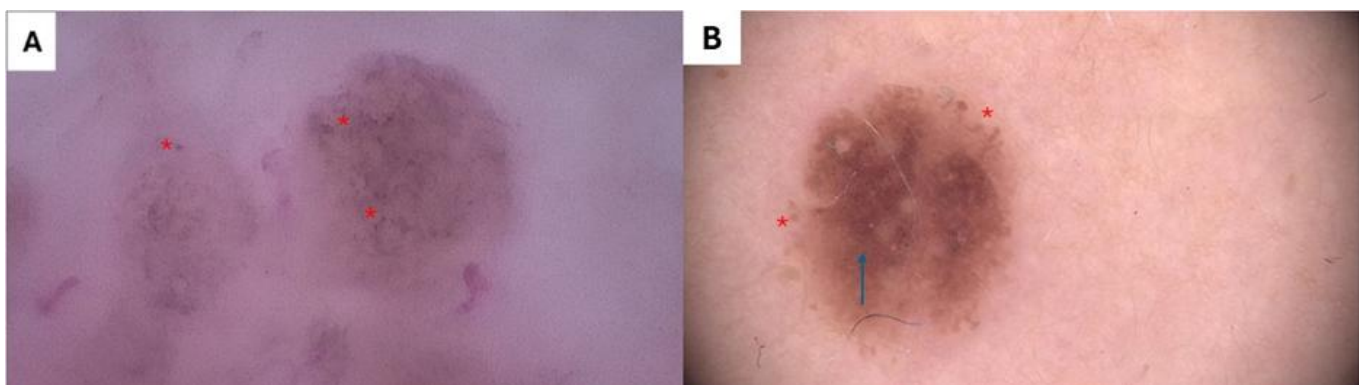


Figure 2: Compound nevi. A. 400X dermoscopy, roundish nests with regular distributed melanocytes B. 20x dermoscopy image, symmetrical peripheral globules (red asterisk) and homogenous pigmentation (blue arrow).

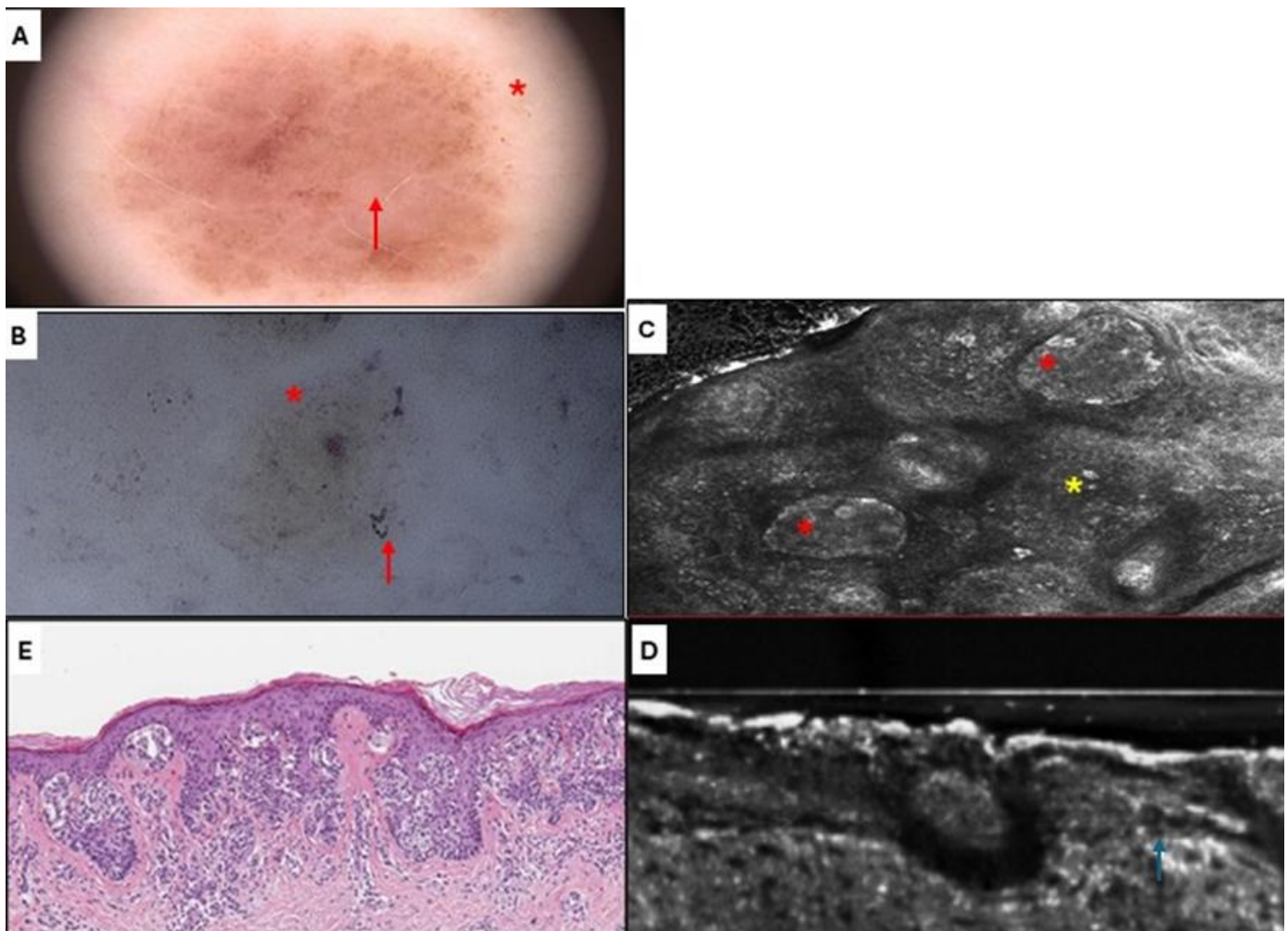


Figure 3: High grade dysplasia. A. 20x dermoscopy, irregular asymmetric globules (red asterisk), regression area (red arrow). B. 400x dermoscopy, sparse nest composed of pleomorphic cells (red asterisk), melanophages: large blue-to-violet non-in-focus cells with a not defined polymorphous shape (red arrow) C. RCM, sparse melanocytes nests (red asterisk), few pleomorphic polygonal atypical cells D. LC-OCT disarranged dermal epidermal junction (blue arrow), E. Histology.

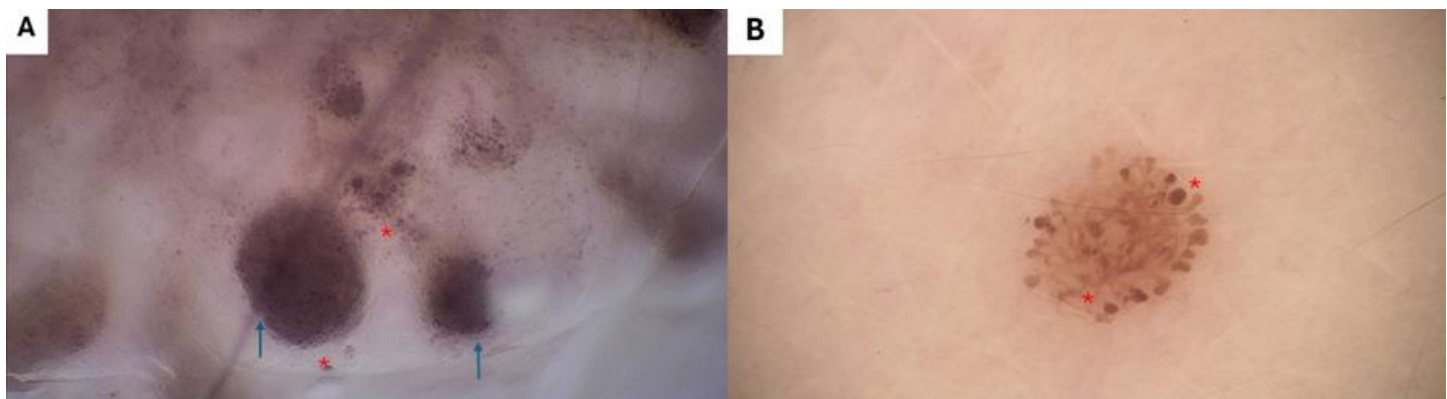


Figure 4: High grade dysplasia. A 400X dermoscopy, roundish nests of melanocytes (blue arrow), scattered polygonal melanocytes (red asterisk) B. 20x dermoscopy, asymmetrical globules with variable size (red asterisk).

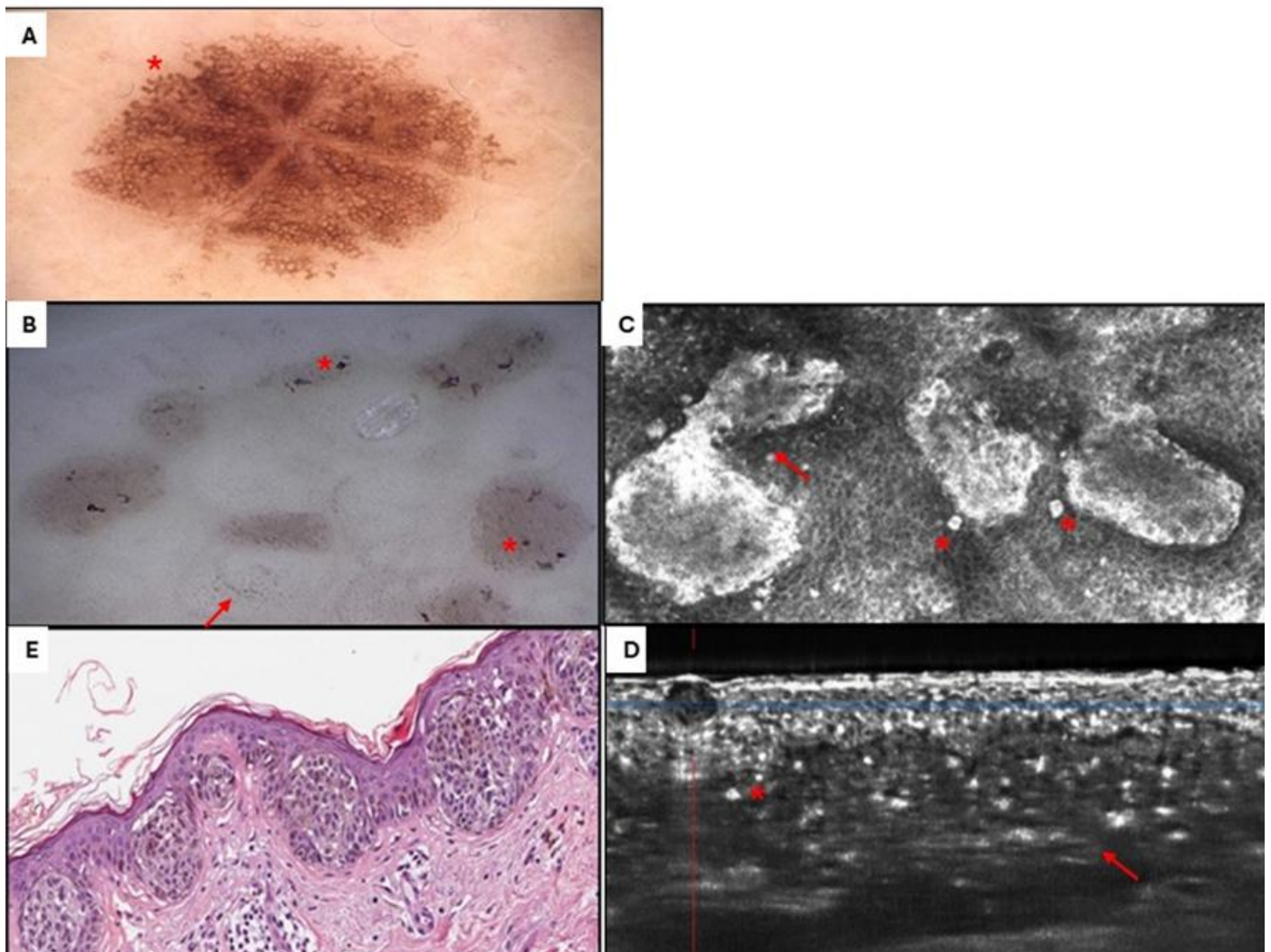


Figure 5: Melanoma. A. 20x dermoscopy, irregular asymmetric globules (red asterisk), B. 400x dermoscopy, round and irregular melanocytes and dendritic melanocytes (red star), irregular vessels (red arrow), C. RCM. Atypical pleomorphic cells in a pagetoid fashion in single units and small aggregates (red star). D. LC-OCT. Atypical pleomorphic cells (red star) disarranged dermal epidermal junction (red arrow) E. Histology.

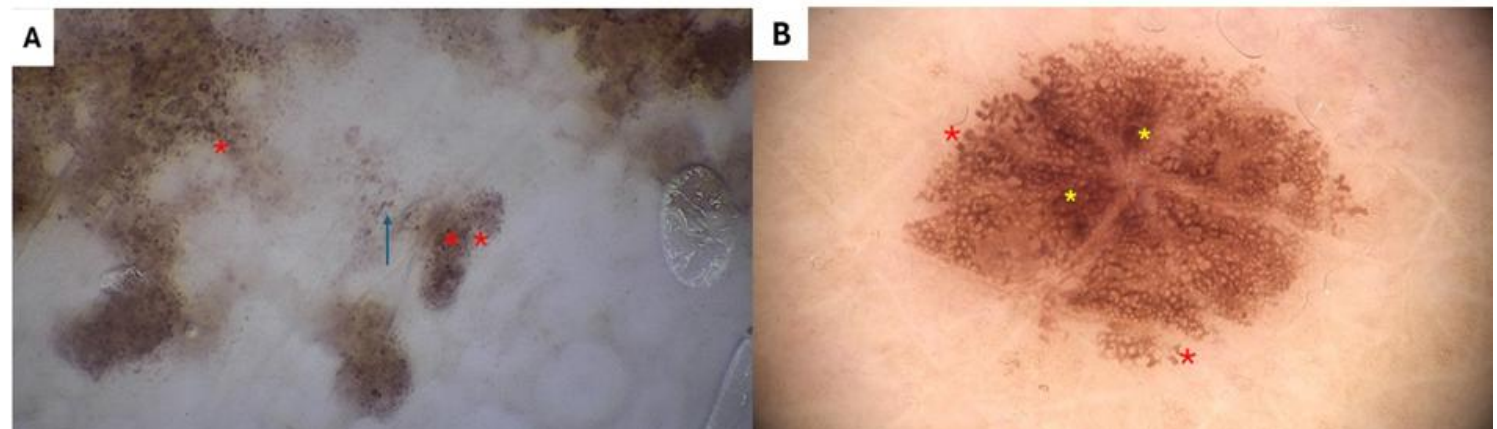


Figure 6: Melanoma. A. 400x dermoscopy, scattered and irregular melanocytes in shape and size (blue arrow), roundish and pleomorphic melanocytes (red asterisk). B. 20 x dermoscopy, asymmetric irregular globules (red asterisk), irregular pigment network (yellow asterisk).

Age (ys)		Total nr (%)
Median (Range) 40 (22-77)		40 (100)
Age < 30y (group I)		6 (15.0)
Age 30-50y (group II)		24 (60.0)
Age >50y (group III)		10 (25)
Phototype		
I		4 (10)
II		23 (57.5)
III		13 (32.5)
Positive cutaneous malignancies family history		11 (27.5)
Sex		
Male		16 (40.0)
Female		24 (60.0)

Table 1: Patients' demographic data.

Age Group	Histology Diagnosis, Total nr (%)				
	Compound Nevi	Atypical Nevi	High Grade Dysplasia	Melanoma	Clark Nevi
I	4 (66.7)	1 (16.7)	0 (0.0)	0 (0.0)	1 (16.7)
II	12 (50.0)	10 (41.7)	0 (0.0)	0 (0.0)	2 (8.3)
III	3 (30.0)	4 (40.0)	1 (10.0)	1 (10.0)	1 (10.0)
Tot	19 (47.5)	15 (37.5)	1 (2.5)	1 (2.5)	4 (10.0)
P-value	0.405				

Table 2: Histological diagnosis depending on age group.

Age Group	Dermoscopy globules variability, Total nr (%)				Dermoscopy globules Asimmetrycal Distribution, Total nr (%)
	Pigmentation	Shape	Size	Tot	
I	2 (33.3)	1 (16.7)	3 (50.0)	6 (19.2)	1 (16.7)
II	4 (16.7)	6 (25.0)	10 (41.7)	20 (60.6)	3 (3.0)
III	2 (10.0)	1 (10.0)	4 (40.0)	7 (21.2)	2 (20.0)
P-value	0.695	0.594	0.918		0.609

Table 3: 10 x dermoscopic globule variability in pigmentation, size and shape and globule asimmetrycal distribution depending on the age group.

Age Group	400 X Dermoscopy Melanocytes Morphology, Total nr (%)					Atypical cellularity, Total nr (%)	
	Round Melanocytes	Dendritic Melanocytes	Round And Dendritic Melanocytes	Roud And Irregular Melanocytes	Tot	LC-OCT	RCM
I	5 (83.3)	0 (0.0)	1 (16.7)	0 (0.0)	6 (15.0)	0 (0)	1 (16.7)
II	22 (91.7)	1 (4.2)	1 (4.2)	0 (0.0)	24 (60.0)	3 (12.5)	5 (20.8)
III	7 (70.0)	0 (0.0)	2 (20.0)	1 (10.0)	10 (25.0)	2 (20)	2 (20.0)
P-value	0.407					0.504	0.974

Table 4: Patients' melanocytes morphology on 400x dermoscopy and atypical cellularity at LC-OCT and RCM depending on age group.

Histologic Diagnosis	Dermoscopy Globule Distribution, Total nr (%)			Dermoscopy Globule Variability, Total nr (%)		
	Eccentric	Asymmetric	Peripheral	Pigmentation	Shape	Size
Compound nevi	4 (44.4)	1 (5.3)	14 (73.7)	6 (31.6%)	3 (15.8%)	8 (42.1%)
Atypical nevi	3 (33.3)	1 (5.3)	11 (73.3)	15 (6.7%)	3 (20.0%)	6 (40.0%)
High grade dysplasia	0 (0)	1 (100)	1 (100)	0 (0.0%)	0 (0.0%)	0 (0.0%)
Melanoma	0 (0)	1 (100)	0 (0)	0 (0.0%)	1 (100.0%)	1 (100.0%)
Clark nevi	2 (22.2)	1 (25.0)	1 (25.0)	1 (25.0%)	1 (25.0%)	2 (50.0%)
P-value	0.664	<0.05	0.107	0.431	0.340	0.695

Table 5: Association between dermoscopic globule distribution and histological diagnosis.

Hystologic Diagnosis	400 x Dermoscopy Melanocytes Morphology, Total nr (%)					Atipycal Cellularity, Total nr (%)	
	Round Melanocytes	Dendritic Melanocytes	Round and Dendritic Melanocytes	Roud and Irregular Melanocytes	Tot	LC-OCT	RCM
Compound nevi	18 (94.7)	0 (0.0)	1 (5.3)	0 (0.0)	6 (47.5)	18 (94.7)	0 (0.0)
Atypical nevi	12 (80)	1 (6.7)	2 (13.3)	0 (0.0)	15 (37.5)	2 (13.3)	5 (33.3)
High grade dysplasia	0 (0.0)	0 (0.0)	1 (100)	0 (0.0)	1 (2.5)	1 (100.0)	1 (100.0)
Melanoma	0 (0.0)	0 (0.0)	0 (0.0)	1 (100.0)	1 (2.5)	1 (100.0)	1 (100.0)
Clark nevi	4 (100.0)	0 (0.0)	0 (0.0)	0 (0.0)	4 (10.0)	1 (25.0)	1 (25.0)
P-value			< 0.05			< 0.05	< 0.05

Table 6: Association between 400x dermoscopy features, LCT-OCT and RCM atypical cellularity and histological diagnosis.

400 x Dermoscopy Melanocytes Morphology	Atipycal Cellularity Total nr (%)	
	LC-OCT	RCM
Round melanocytes	3 (60.0)	6 (75.0)
Dendritic melanocytes	0 (0.0)	0 (0.0)
Round and dendritic melanocytes	1 (20.0)	1 (12.5)
Roud and irregular melanocytes	1 (20.0)	1 (12.5)
Tot	5 (100.0)	8 (100.0)
P-value	< 0.05	0.219

Table 7: Correlation between 400 x dermoscopic features and RCM and LC-OCT atypical cellularity.

Discussion

The objective of this study was to assess the prognostic significance of the peripheral globular pattern in melanocytic nevi using a multimodal, non-invasive diagnostic approach including low- and high-magnification dermoscopy, RCM and LC-OCT. We enrolled 40 adult patients (≥ 22 years old), of both sexes, attending the Dermatology Unit at the Spedali Civili Hospital in Brescia (Italy) between February 16 and September 30, 2023, all of whom presented PGN with peripheral globules on traditional dermoscopy. The comprehensive results obtained in this study offer a detailed overview of how patient characteristics, dermoscopic features and non-invasive imaging findings correlate in PGN. Notably, the majority of PGN cases occurred in patients aged 30–50, with a predominance in females. This trend is consistent with prior studies [4–6]. Among patients younger than 30, the most common histopathologic diagnosis was compound nevus, followed by atypical nevus and Clark's nevus. However, given the small number of patients in this group ($n = 6$), meaningful conclusions are limited. The chi-square analysis ($\chi^2 = 8.296$; $df = 8$; $p = 0.405$) did not reveal a statistically significant association between patient age and histologic diagnosis. In the 30–50 age group, compound nevi remained the most frequent diagnosis, followed by atypical and Clark's nevi. In patients older than 50, a broader diagnostic spectrum was observed, including atypical nevi and melanoma. Nonetheless, small sub group sizes may have limited statistical power. Overall, the data suggest a possible age-related trend in histologic outcomes, with more severe diagnoses occurring in older patients. However, no strong statistical association was demonstrated between age group and histopathologic diagnosis. Notably, the presence of large globules was significantly more common in patients over 50. To

our knowledge, no previous study has reported a correlation between globule size and patient age. In contrast, features such as asymmetry in globule distribution and globule shape variability did not appear to be influenced by age. When correlating dermoscopic, RCM and LC-OCT features with histology, several important associations emerged. Asymmetric distribution of peripheral globules was strongly associated with more concerning diagnoses such as melanoma and severely dysplastic nevus and this feature was observed in 100% of melanoma and severely dysplastic nevus cases.

Peripheral distribution of globules alone was less discriminative, although it was relatively uncommon in Clark's nevi (25.0%). Variability in globule size and shape was notably associated with the melanoma case (100%), whereas pigment variability appeared more frequently in compound nevi (31.6%). Melanocyte morphology under 400x magnification was also informative: irregular melanocytes were detected only in the melanoma case.

Atypical cellularity identified via LC-OCT and RCM correlated with more severe diagnoses, particularly melanoma and dysplastic nevi, reinforcing their diagnostic value. The correlation between atypical cellularity detected via LC-OCT and that observed via RCM was strong and statistically significant. All five patients with atypical LC-OCT findings also exhibited atypical features on RCM. These findings suggest that the two modalities may serve as complementary tools in the non-invasive assessment of melanocytic lesions. In conclusion, this analysis provides a comprehensive evaluation of the interplay between age, dermoscopic patterns and advanced imaging features in PGN. The findings have practical implications for the early identification and management of high-risk lesions. While this pilot study is limited by its relatively small sample size and monocentric nature, the observed associations underscore the potential value of multimodal, non-invasive diagnostics in stratifying the biological behavior of PGN. Further multicentre studies with larger cohorts are warranted to confirm these results and explore regional or institutional differences in PGN characterization and prognosis.

Conclusion

This study provides new insights into the diagnostic evaluation of melanocytic nevi with a peripheral globular pattern, challenging the long-standing assumption that this feature is exclusively indicative of benignity. First of all, among the 10x dermoscopic globules characteristics observed, globules asymmetric distribution proved to be the most significant to look at, being associated with melanoma and severely dysplastic nevus diagnosis; furthermore the single melanoma case found in our study showed dermoscopic variability in the shape and size of globules. The findings obtained through conventional dermoscopy can be further enhanced by incorporating high-magnification dermoscopy (400x), Reflectance Confocal Microscopy (RCM) and Line-Field Confocal Optical Coherence Tomography (LC-OCT) into the diagnostic workflow, we were able to identify subtle structural abnormalities that may not be readily apparent with conventional dermoscopy alone. Considering the 400x analysis of the lesions, our study showed how irregular melanocyte morphology was significantly associated with melanoma suggesting how this feature should be subjected to careful observation. The collected data showed that the atypical cellularity detected by RCM and LC-OCT was found in cases of melanoma and high-grade dysplastic nevi. Moreover, the concordance between the results of these two techniques was evident, highlighting how the integration of both tools represents a valuable asset for diagnosis. In conclusion, our results demonstrate that asymmetrical globule distribution, irregular pigment networks, pagetoid melanocyte spread on RCM and dermal-epidermal disorganization on LC-OCT were significantly associated with lesions later confirmed as dysplastic nevi with moderate-to-severe atypia or early melanomas. These findings underscore the need for a multimodal diagnostic approach when evaluating melanocytic nevi with a peripheral globular pattern, particularly in cases where standard dermoscopy does not provide a clear distinction between benignity and malignancy.

Future Directions

Given the increasing availability of advanced non-invasive imaging technologies, future research should focus on validating these findings in larger, multi center cohorts and developing automated Artificial Intelligence (AI) models that can assist in quantifying risk factors associated with melanocytic lesions. Additionally, long-term follow-up studies are needed to better understand the natural evolution of nevi with a peripheral globular pattern and to determine whether specific imaging biomarkers can predict malignant transformation over time.

Conflicts of Interest

The authors declare no conflict of interest in this paper.

Funding

None

Authors' Contributions

All authors contributed to conceptualization, treatment execution, manuscript writing and final approval.

References

1. Cappilli S, Ribero S, Cornacchia L, Catapano S, Del Regno L, Quattrini L, et al. Melanocytic lesions with peripheral globules: proposal of an integrated management algorithm. *Dermatol Pract Concept*. 2023;13(1):e2023010.
2. Xu J, Gupta K, Stoecker WV, Krishnamurthy Y, Rabinovitz HS, Bangert A, et al. Analysis of globule types in malignant melanoma. *Arch Dermatol*. 2009;145(11):1245-51.
3. Cinotti E, Tognetti L, Campoli M, Liso F, Cicigoi A, Cartocci A, et al. Super-high magnification dermoscopy can aid the differential diagnosis between melanoma and atypical naevi. *Clin Exp Dermatol*. 2021;46(7):1216-22.
4. Carbone A, Persechino F, Paolino G, Cota C, Piemonte P, Franceschini C, et al. Enlarging melanocytic lesions with peripheral globular pattern: a dermoscopic and confocal microscopy study. *Ital J Dermatol Venereol*. 2021;156(4):467-72.
5. Pampín-Franco A, Gamo-Villegas R, Floristán-Muruzábal U, Pinedo-Moraleda FJ, Pérez-Fernández E, López-Estebaranz JL. Melanocytic lesions with peripheral globules: results of an observational prospective study in 154 high-risk melanoma patients under digital dermoscopy follow-up evaluated with reflectance confocal microscopy. *J Eur Acad Dermatol Venereol*. 2021;35(5):1133-42.
6. Ribero S, Argenziano G, Di Stefani A, Guidante M, Moscarella E, Peris K, et al. Likelihood of finding melanoma when removing a melanocytic lesion with peripheral clods. *J Eur Acad Dermatol Venereol*. 2020;34(12):e812-4.

Journal of Dermatology Research

Publish your work in this journal

Journal of Dermatology Research is an international, peer-reviewed, open access journal publishing original research, reports, editorials, reviews and commentaries. All aspects of dermatological health maintenance, preventative measures and disease treatment interventions are addressed within the journal. Dermatologists and other researchers are invited to submit their work in the journal. The manuscript submission system is online and journal follows a fair peer-review practices.

Submit your manuscript here: <https://athenaeumpub.com/submit-manuscript/>